Exposing metal and silicate charges to electrical discharges: Did chondrules form by nebular lightning?

Carsten Güttler [a,*], Torsten Poppe [a], John T. Wasson [b], Jürgen Blum [a]

[a] *Institut für Geophysik und extraterrestrische Physik, Technische Universität Braunschweig*
[b] *Institute of Geophysics and Planetary Physics, University of California, Los Angeles*

Abstract

In order to investigate the hypothesis that dust aggregates were transformed to meteoritic chondrules by nebular lightning, we exposed silicatic and metallic dust samples to electric discharges with energies of 120 to 500 J in air at pressures between 10 and 10^5 Pa. The target charges consisted of powders of micrometer-sized particles and had dimensions of mm. The dust samples generally fragmented leaving the major fraction thermally unprocessed. A minor part formed sintered aggregates of 50 to 500 μm. In a few experiments melt spherules having sizes $\lesssim$ 180 μm in diameter (and, generally, interior voids) were formed; the highest spherule fraction was obtained with metallic Ni. Our experiments indicate that chondrule formation by electric current or by particle bombardment inside a discharge channel is unlikely.

Key words: chondrules, meteorites, lightning, solar nebula, origin, planetary formation, method: laboratory

1. Introduction

Chondrules are millimeter-sized spheroids which are common in primitive chondritic meteorites and formed by melting and resolidification in the early solar system some 4.56 Myrs ago. Consisting mainly of FeO- and MgO-rich silicate minerals, most chondrules are porphyritic, have experienced two or more melting events, and were incompletely melted in the final melting event (Wasson and Rubin, 2003). From their abundance and their various characteristics chondrules provide the key to fascinating insights into the early solar system.

The process which formed chondrules is still unknown. It must have been very energetic and is thus in striking contrast to the low energetic protoplanetary coagulation of dust, presumably taking place at the same time. Many hypotheses of chondrule formation processes are listed by Boss (1996), and although recent works favor the formation in nebular shocks or X-wind jets (see Ciesla, 2005), the formation in nebular lightning which was originally proposed by Whipple (1966) is still under serious discussion.

The idea of the lightning hypothesis is that dust in the solar nebula underwent tribocharging in non-sticking collisions, and a subsequent spatial separation lead to large-scale electric fields which finally caused an electrical breakdown. Inside this discharge channel preexisting clumps of solid particles were heated, either by the passage of electric currents, by the bombardment of surfaces by energetic particles, or by electromagnetic radiation (Horányi et al., 1995). Outside the channel, radiation emitted by the hot plasma (Wasson, 1996; Eisenhour et al., 1994; Eisenhour and Buseck, 1995), thermal exchange with the heated gas or recombination of atomic H on the chondrule surfaces as compiled by Desch (2000) may have lead to the formation of chondrules.

There is extensive former work on the lightning hypothesis (e.g. Morfill et al., 1993; Horányi et al., 1995; Gibbard et al., 1997; Pilipp et al., 1998; Desch and Cuzzi, 2000), whereas recent works disregard the idea mainly because cooling times in this environment are thought to be too fast to form the observed chondrule textures. Contrariwise, lightning models are supported by some researchers who have inferred the very cooling times on a scale of seconds (e.g. Greenwood and Hess, 1996; Wasson and Rubin, 2003). Remanent magnetization of chondrules is furthermore discussed to be a hint that chondrules formed in regions with high magnetic fields which could result from lightning (Wasilewski and Dickinson, 2000; Acton et al., 2007).

---

* Corresponding author.

Email address: `c.guettler@tu-bs.de` (Carsten Güttler).

Related to our work presented below, it is important that electrical charge is effectively separated to establish high potentials for lightnings with sufficient energy to melt chondrules (Desch and Cuzzi, 2000). Sufficiently high charge transfers (not the tribocharge mechanism) were in fact confirmed by experimental investigations of collision-induced charging of micrometer sized grains (Poppe and Schräpler, 2005; Poppe et al., 2000).

In this research we followed a procedure similar to that described by Wdowiak (1983), who exposed a mm-sized dust ball of Allende meteoritic material to a 5 kJ electric discharge. His experiments left most material unprocessed, produced some sintered agglomerates, and a few spherules in the size range of 100 to 200 μm containing bubbles in the interior and on the surface. He concluded that chondrules did not form by lightning.

In our experiments we exposed dust agglomerates to an electrical discharge between electrodes. We varied sample material, pressure, and discharge energy, and we made quantitative analysis of spherule size distribution and energetic efficiencies of the melt processes.

Section 2 describes the experimental setup and all experimental parameters, and in section 3 the results are presented. Energetic efficiency, stability of dust aggregates, the porosity of melt spherules and possible consequences of aggregate sintering are discussed in section 4 and concluded in section 5.

2. Experimental setup

We used a vacuum chamber suitable for air pressures between 10 and 10^5 Pa which contained two electrodes made of silver-coated copper wires separated by a typical distance of 3 mm. The electrodes were electrically connected to a $5\,\mu$F capacitor which could be charged to $7-14$ kV resulting in a total electric energy between 123 and 490 J. This setup determined a discharge duration of approximately 60 μs as measured with a photodiode. The maximum light intensity is reached after a few microseconds, and so is the maximum temperature. This was measured by two-color photometry which provided an estimation of maximum temperature of 6500 K (emission lines were not taken into account). The ambient gas in all experiments was air.

Dust powder samples of about 1 mm in size (approx. $1-5$ mg, consisting of micrometer-sized grains; cf Table 1) were placed on a plastic (PVC) sample holder between the electrodes as illustrated in Fig. 1.

To avoid contamination of the sample, the electrodes were replaced after each experiment. No erosion or melting was observed on the plastic sample holder and the chamber could easily be cleaned to avoid contamination with samples of preceding experiments.

For a qualitative analysis, the processed dust sample was collected on a glass plate on the bottom of the chamber and then examined with optical or scanning electron microscopy (SEM). Some target materials formed spherules
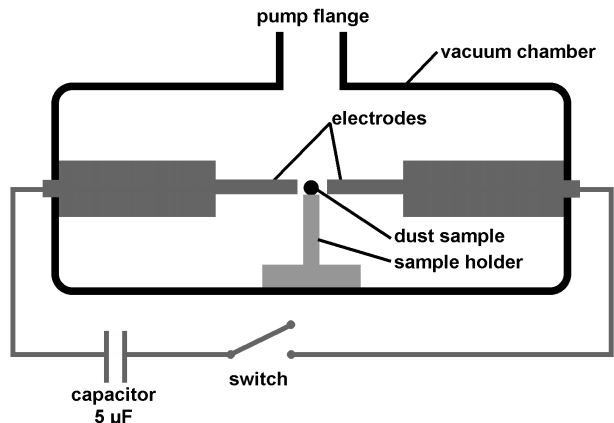

Fig. 1. Sketch of the experimental setup. The dust sample is placed between two electrodes in a vacuum chamber.

which could be embedded into epoxy resin for sectioning. For quantitative analysis of the melt spherules, the sample was collected on a sheet of paper and then put into a mold of 1×1 cm. This mold was then scanned by light microscopy for counting the spherules and measuring their sizes.

Charges were composed of fayalite, forsteritic olivine, SiO_2, iron (oxidized on the surface), and nickel as described in Table 1. Some studies were carried out on peridotite 699 collected by G. Witt-Eickschen at Schönfeld, West Eifel, Germany. It has the following chemical composition: SiO_2, 44.14 %; Al_2O_3, 3.07 %; FeO, 7.17 %; MgO, 40.93 %; CaO, 2.8 % and Na_2O, 0.29 %. The Mg/Mg+Fe molar ratio is 0.912. Other similar samples were discussed in the paper by Witt and Seck (1987). The choice of materials was lead by the idea of clean and defined conditions to enable repeatability and moreover the peridotite is directly compositionally relevant. Furthermore, the conductivity of nickel and iron must play a role in electric discharge and the SiO_2 monomers have already been used in sintering experiments (Poppe, 2003) and are well analyzed (Heim et al., 1999) to permit calculations.

3. Results

3.1. Phenomenology of processed material

Instantly after triggering the discharge, the dust sample exploded. This happened at all pressures, discharge energies, and sample materials. However, small parts of the samples were thermally processed and could afterwards be found on the glass plate. Apart from unprocessed, dispersed dust, sintered dust agglomerates ($50-500$ μm in diameter) were common and, depending on the material, also spherules (diameter $\lesssim$ 180 μm) were found. Iron powder showed the most product variety including hollow spheres and millimeter-sized, comparatively dense agglomerates. Figure 2 shows a variety of processed dust samples found after discharge heating. Experimental parameters and outcomes are compiled in Table 2. To guarantee reproducibil-

Table 1

Material parameters of selected dust types. The properties for the San Carlos Olivine are calculated by assuming 9 % Fayalite and 81 % Forsterite. Sources: [a]manufacturer information (goodfellow.com), [b]Lide (1998), [c]Wasson (1996), [d] calculated from melting temperature, specific heat capacity, and heat of fusion, [e]Schön (1996)

|	nickel	iron	fayalite	San Carlos olivine	silica
density [g cm^{-3}]	8.9[a]	7.87[a]	4.30[b]	3.3[b]	2.18 − 2.65[b]
melting temperature [$^{\circ}$C]	1453[a]	1535[a]	1490[c]	1861[b,c]	1713[b]
spec. heat capacity[b] [J g^{-1} K^{-1}]	0.444	0.449	0.652	0.825	0.738
heat of fusion [J g^{-1}]	292[a]	272[a]	452[c]	500[b,c]	142[b]
tot. spec. heat[d] [J g^{-1}]	928	952	1410	1808	1391
heat conductivity [W m^{-1} K^{-1}]	90.7[b]	80.2[b]	3.0[e]	5.7[e]	1.35[b]
el. resistivity [$\mu\Omega\cdot$cm]	6.9[a]	10.1[a]			
grain size [μm]	0.2 − 5	0.1 − 1.2	< 50	< 50	0.9 − 1.7
mean grain size [μm]	2.33	0.56	0.75	1.43	1.26
mean axis ratio	1.16	1.15	1.59	1.57	1.15
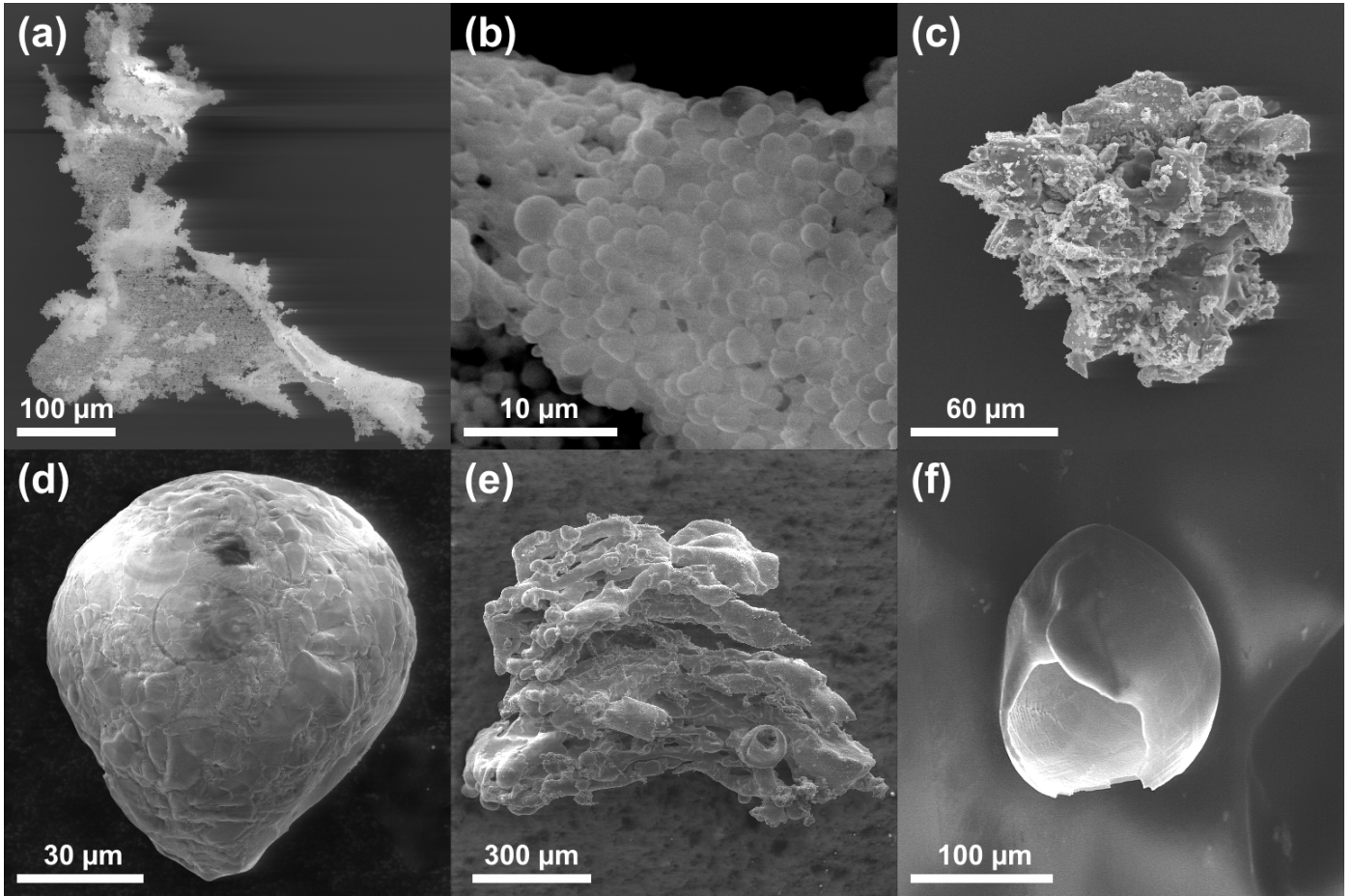
Fig. 2. Typical experimental outcomes: (a) Sintered agglomerate of SiO$_2$ monomers, (b) magnified SiO$_2$ agglomerate, (c) sintered agglomerate of fayalite grains, (d) nickel spherule (e) iron agglomerate and (f) hollow iron sphere.

ity, all specified experiments were conducted at least three times. Hence, the results presented in the following are representative for a series of experiments with same materials and parameters.

Sintered agglomerates like Fig. 2 (a) – (c) formed from silicates and nickel with all experimental parameters. Figure 2 (b) indicates that the energy transferred to the sample was insufficient to completely melt the SiO$_2$ powder. The original 1 μm silica spheres were sintered to a varying ex-

tend as can be concluded from similar structures found in sintering experiments by Poppe (2003). Due to preparation in a ball mill, the fayalite grains varied much more in size and shape but sintering is nevertheless suggested from Fig. 2 (c) which shows an aggregate partly consisting of rounded shapes and partly of grains with original sharp edges and of original grain size. For all parameters tested (Table 2), peridotite and olivine powder only formed sintered agglomerates looking similar to the fayalite agglomerate in Fig. 2

Table 2
Experiment results for different parameters. If spherules are formed, agglomerates of sintered ("sintered") grains are also common. Exception: Iron charges formed dense aggregates which do not resemble the original grains ("big agglomerate"). Unprocessed dust was always present.

discharge energy, gas pressure	iron	peridotite 699	fayalite	olivine	silica	nickel
456 J, 10^5 Pa	big agglomerate, hollow spherules		porous spherules	sintered	sintered	porous spherules
456 J, 10^3 Pa	spherules	sintered			sintered	
141 J, 10 Pa	spherules	sintered	sintered	sintered		sintered
456 J, 10 Pa	spherules	sintered	sintered	sintered	sintered	sintered

(c). Some spherules were found in experiments with nickel and fayalite powder at 10^5 Pa and also for iron at pressures below 10^3 Pa. Due to their similarity only one exemplary nickel spherule is presented in Fig. 2 (d). For pressures below 10^5 Pa, nickel powder only formed sintered aggregates $\lesssim 80\ \mu$m in size, resembling the SiO_2 aggregate in Fig. 2 (a) and (b). In each experiment with iron powder at 10^5 Pa gas pressure, one or two dense agglomerates of $\sim$1 mm were formed as shown in Fig. 2 (e). These agglomerates did not form by sintering the original iron grains as can be seen from the thickness of the substructures ($\sim$30 μm) which are larger than the original grain size (spheres of $0.1 - 1.2\ \mu$m). Figure 2 (f) shows a hollow sphere of $\sim 150\ \mu$m with a wall thickness of only some 10 μm, which formed from iron powder together with those dense agglomerates in Fig. 2 (e).

3.2. Quantitative analysis of spherules

For some of our experimental parameters, spherules were found. Nickel and fayalite formed spherules at 10^5 Pa air pressure as shown in Fig. 2 (d) for nickel. Fayalite as well as nickel spherules show a varying porosity from 0 to 60 % (cf. Fig. 3). The mean porosity computed from 11 fayalite spherules and 19 nickel spherules was 49 ± 4 % and 5.2 ± 1.7 %, respectively. Solid iron spherules were found for pressures $\lesssim 10^3$ Pa whereas all iron spherules formed at 10^5 Pa were hollow bubbles as can be seen from the example in the SEM image in Fig. 2 (f).

In addition to examining single spherules, the number and size distribution of spherules produced in individual experiments were determined for the experiments in which spherules formed. The sizes were binned, cumulated, and plotted with a logarithmic number-axis (Fig. 4). The resulting straight line suggests an exponential behavior $\tilde{N}(R) = a \cdot \exp(-bR)$, where R is the spherule radius, $\tilde{N}$ is the number of counted spherules of radius $\geq R(\tilde{N})$ and a and b are fitting parameters. Figure 4 shows these size distributions for all three conditions under which spherules were found. The range of spherule sizes used for the fit was limited to spherules $> 5\ \mu$m because smaller spherules were poorly resolved on the images. The value $R_{max} = \frac{3}{b}$ defines the radius of spherules which contain the most mass for one given distribution because it gives the maximum of the function $N(R) \sim R^3 \cdot e^{-bR}$. This radius was found to be approximately 40 μm for fayalite and nickel spherules and 16 μm for iron spherules (cf. Table 3).
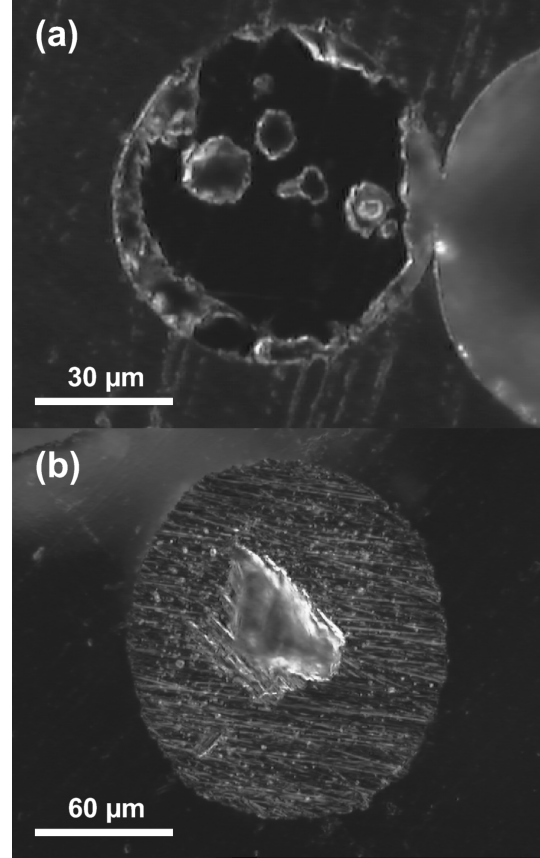

(a)

30 µm

(b)

60 µm

Fig. 3. Embedded and sectioned spherules made at 10^5 Pa and 490 J. (a) Fayalite spherule with a measured porosity of 14 % and (b) nickel spherule with a porosity of 11 %.

Table 3
Total mass in spherules and R_{max} for all experiments in which the spherules were counted (discharge energy 456 J).

material	pressure	total mass	R_{max}
	[Pa]	[μg]	[μm]
fayalite	10^5	23.6	44.2
fayalite	10^5	38.9	36.0
iron	10	18.2	20.9
iron	10	4.6	13.1
iron	10	13.4	19.4
iron	10	9.9	12.4
nickel	10^5	319.6	40.4

Furthermore the total mass transformed into spherules was calculated by summing the mass of all counted spherules, taking into account the measured mean porosity depending on the material. According to this, the mass
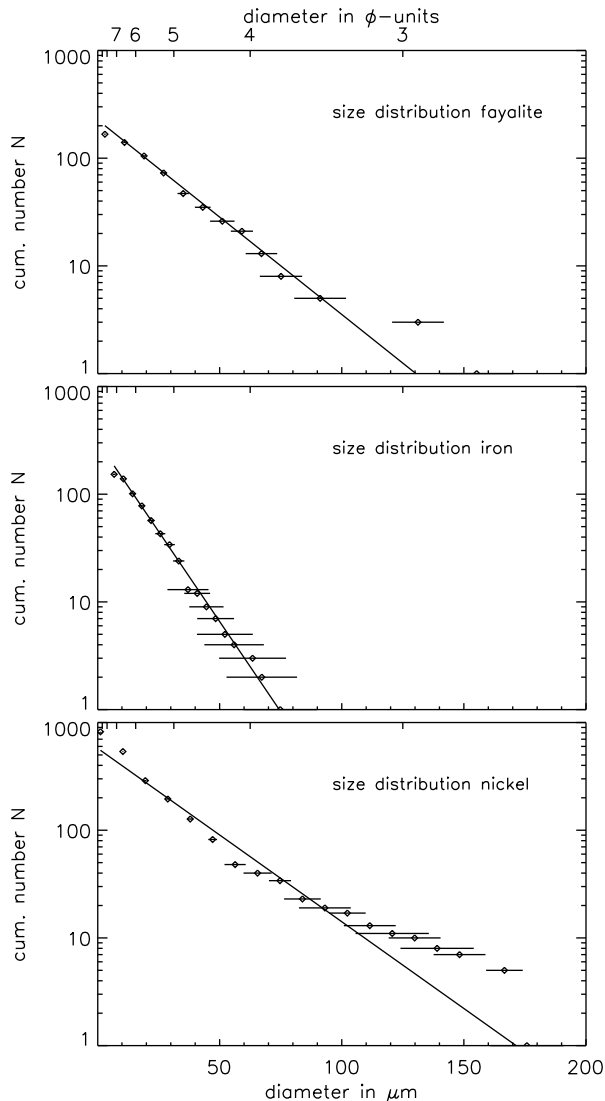
Fig. 4. Cumulative size distribution for all counted spherules in one experiment. From top to bottom: Fayalite, iron, and nickel.

that was transformed into spherules is 31 μg for fayalite, 12 μg for iron, and 320 μg for nickel powder (cf. Table 3). The total energy for melting these masses can be deduced using Table 1. It is thus possible to provide an energetic efficiency of discharge melting which is the fraction of energy consumed for melting divided by the input electrical discharge energy. We find an energetic efficiency of 0.006 % (fayalite), 0.004 % (iron) and 0.06 % (nickel).

3.3. *Pre-sintered aggregates in the discharge*

In order to assess the force driving the fragmentation, pre-sintered dust aggregates of SiO_2 powder have been put into the discharge. These were similar to aggregates described by Poppe (2003) and were sintered in a furnace for one hour at 1050°C and 1100°C, respectively.

The agglomerates which were sintered at 1050°C frag-

mented, were completely dispersed, and were thermally unprocessed whereas those sintered at 1100°C were stable but did also not melt. The tensile strength of a macroscopic sintered aggregate is unknown but the neck radius between single monomers, giving an indication for the bondings, was measured by Poppe (2003) to 0.4 (1050°C) and 0.55 (1100°C) of the particle radius.

4. Discussion

4.1. *Agglomerate destruction and melt spherule sizes*

Under all experimental conditions, most of the dust sample was dispersed rather than thermally processed. Wdowiak (1983) made similar observations but, unfortunately, did not provide details. We exclude electrical forces as cause of dust fragmentation (see appendix A). Instead, we attribute the explosion to the expansion of the discharge channel, possibly supported by evaporation of volatile materials, both processes dependent on the discharge temperature. There is no indication that hypothetical nebular lightning discharges had lower temperatures than our experimental discharge, in most models much higher temperatures are inferred (Horányi et al., 1995). Thus, nebular lightning should have been even more violent than our experiments. So in nebular lightning, loosely-bound aggregates of micrometer-sized grains would not have survived within the discharge channel. If spherules were formed, the heating must thus have been by above mentioned processes outside the high-temperature channel.

Nevertheless, a few melt spherules were produced in our experiments, but they amount a very small fraction of the original material and are, in most cases, smaller than chondrules. It is thus obvious that some small fragments of the original sample were melted. Because we know so little about nebular lightning and the various processes by which it could cause dust to melt, it is difficult to generalize further.

4.2. *Energetic efficiency*

While the question whether nebular lightning could have had as much energy as necessary to melt chondrules has been treated (Desch and Cuzzi, 2000), the question how effective lightning energy is for melting has not yet been discussed. The ultimate energy source for a possible chondrule melting by lightning is potential energy of disk material in the gravitational field of the sun. At 2 AU, this specific energy is $E = \gamma M_\odot / r = 4 \cdot 10^8$ J kg^{-1} whereas the required energy for the complete fusion of silicates like fayalite is at least $1.5 \cdot 10^6$ J kg^{-1} (cf. Table 1). Taking into account at least two heating cycles (Wasson, 1993, 1996) this leads to a lower limit of an efficiency of ~ 1 % necessary to melt chondrules under the unrealistically favorable condition that all potential energy is converted into electric lightning energy. Even then, the efficiency found in

the experiments is lower by more than one order of magnitude, and this is only true for nickel at 10^5 Pa (fayalite and iron two orders of magnitude). So the energetic efficiency is much too low in order to explain chondrule formation by particle bombardment heating or electrical current heating inside nebular lightning channels. However, our results do not exclude other heating mechanisms as discussed in introduction. E.g., nebular lightning heating by electromagnetic radiation could have been stronger than in our experiments due to different length scales. A possible step forward to treat the problem of radiation heating could be experiments on dust aggregate melting by laser radiation (Springborn et al. in preparation).

We find a clear trend that conductive materials are more easily melted in the experimental discharge than nonconductive: Nickel has the highest energetic efficiency of all used powders and apart from the moderate efficiency in forming solid spherules, also the iron powder shows a high processing rate in forming one big agglomerate. Fayalite is the only nonconducting powder which melted at all. Possible reasons for the greater melting of the conductors may be the heating by interior currents and the focusing of electric flux lines followed by an increased number of bombarding charged particles. From this we conclude that the conductive fraction of chondrule precursor material would have played an important role in a formation process with heating by nebular lightning.

4.3. *Porosity*

Most nickel and fayalite spherules were porous. In fayalite spherules bubbles made up 49 % of volume on average, and, in nickel spherules it was 5 %. Since bubbles are rarely observed in chondrules their presence in our products seems to be an argument against chondrule formation in nebular discharges, as also noted by Wdowiak (1983). However, this argument is not strong as it has been recognized that bubble retention could be a consequence of low energetic efficiency which resulted in a low degree of melting. Maharaj and Hewins (1993) argue that bubbles are typical for a low degree of melting because viscosity is temperature dependent such that at low temperatures bubbles cannot escape as easily as at high temperatures. This is consistent with the finding that fayalite has a lower energetic efficiency than nickel and also a higher porosity. A higher energetic efficiency might therefore lead to a higher degree of melting and hence to a lower porosity.

4.4. *Other aspects*

We found that experiments more often resulted in sintering and strengthening of agglomerate fragments than in melt spherule formation. Therefore, other effects of possible nebular lightning on pristine solar nebula material should also be considered. An obvious link could exist to protoplanetary dust aggregation for which the collisional behav-

ior, and thus the strength, of growing agglomerates is a key question (Blum and Wurm, 2008). Collision experiments with well defined sintered dust agglomerates (Poppe, 2003) are ongoing to study their behavior (Krause and Blum, pers. comm.). In turn, also the search for features of sintering in primitive solar system material could give indications wether lightning occurred in the solar nebula or not.

5. Conclusion

We performed experiments on electrical discharge heating of micrometer-sized silicatic and metallic dust powder in order to investigate the hypothesis that chondrules may have formed by lightning in the solar nebula. We found that discharge heating is energetically extremely inefficient in our experiments. Dust aggregates were destroyed instead of transformed into melt spherules. The few spherules produced were smaller than meteoritic chondrules and, in contrast to them, much more porous.

While it is true that some spherules had the size of small chondrules and porosity may be a consequence of low energetic efficiency, aggregate destruction and low energetic efficiency are strong and independent arguments against chondrule formation inside nebular lightning channels. Any theory on chondrule formation in nebular lightning discharges must explain why nebular lightning did not destroy chondrule precursor aggregates and must also deal with the low energetic efficiency. However, other lightning-related heating mechanisms outside the lightning channel are not excluded by the results of our experiments.

The experiments showed however that if lightning occurs in the early solar system at all, it will be able to alter dust agglomerates with possible consequences to protoplanetary dust growth.

Appendix A. Estimation of agglomerate destruction effects

The order of magnitude for thinkable electric effects which can lead to the fragmentation of a dust aggregate are hereafter estimated: *(i)* Electrostatic repulsion and *(ii)* forces due to field gradients will be calculated for 1 μm SiO_2 monomers because of their well-known material parameters (Heim et al., 1999; Blum and Schräpler, 2004).

(i) The Coulomb force between two charged grains in contact is $F = (Ze)^2/(4\pi\varepsilon_0 D^2)$, where Z is the number of electrons of charge e on each grain and $D = 1$ μm is the distance of the grain centers. The charge on each grain must be 17,000 elementary charges to overcome the adhesive force of 67 nN measured by Heim et al. (1999) and lessens only slightly for a chain of charged grains.

(ii) If a chain of SiO_2 spheres is equally charged, the force due to the difference in the electric field on the one end to the other may break it. This happens when the repulsive force $F = ZeE'D\frac{n(n+1)}{2}$ is stronger than the adhesive force of 67 nN, where n is the number of monomers in a chain and

E' is the gradient in the electric field in V/m^2. One case in the experiment with the lowest field gradient in which the sample still fragmented is for an electrode distance of 35 mm and a potential difference of 13.5 kV between the electrodes, which results in a field gradient of 10^5 V/m^2 at the edge of the dust sample. Assuming a chain of 10 monomers on the surface which are equally charged, $8 \cdot 10^{10}$ elementary charges had to be deposited on each monomer to overcome the adhesive force of 67 nN.

Horányi et al. (1995) calculated the charge on a mm-sized dust ball in a 30 eV hot plasma to $5 \cdot 10^7$ electrons, which leads to only 10 charges per monomer assuming that the aggregate is porous and only surface layers are charged. This is much too little for both electrical effects.

References

Acton, G., Yin, Q.-Z., Verosub, K. L., Jovane, L., Roth, A., Jacobsen, B., Ebel, D. S., Mar. 2007. Micromagnetic coercivity distributions and interactions in chondrules with implications for paleointensities of the early solar system. Journal of Geophysical Research (Solid Earth) 112, 3.

Blum, J., Schräpler, R., Sep. 2004. Structure and Mechanical Properties of High-Porosity Macroscopic Agglomerates Formed by Random Ballistic Deposition. Physical Review Letters 93 (11), 115503.

Blum, J., Wurm, G., 2008. The Growth Mechanisms of Macroscopic Bodies in Protoplanetary Disks. Annual Review of Astronomy and Astrophysics, in press.

Boss, A. P., 1996. A concise guide to chondrule formation. In: Hewins, R., Jones, R., Scott, E. (Eds.), Chondrules and the Protoplanetary Disk. pp. 257–263.

Ciesla, F. J., 2005. Condrule-forming processes – an overview. In: Krot, A. N., Scott, E. R. D., Reipurth, B. (Eds.), Chondrites and the Protoplanetary Disk. pp. 811–820.

Desch, S. J., Mar. 2000. Astrophysical Constraints on Chondrule Formation Models. In: Lunar and Planetary Institute Conference Abstracts. Vol. 31 of Lunar and Planetary Institute Conference Abstracts. p. 1923.

Desch, S. J., Cuzzi, J. N., 2000. The generation of lightning in the solar nebula. Icarus 143, 87–105.

Eisenhour, D. D., Buseck, P. R., Sep. 1995. Chondrule formation by radiative heating: A numerical model. Icarus 117, 197–211.

Eisenhour, D. D., Daulton, T. L., Buseck, P. R., Aug. 1994. Electromagnetic Heating in the Early Solar Nebula and the Formation of Chondrules. Science 265, 1067.

Gibbard, S. G., Levy, E. H., Morfill, G. E., Dec. 1997. On the Possibility of Lightning in the Protosolar Nebula. Icarus 130, 517–533.

Greenwood, J. P., Hess, P. C., 1996. Congruent melting kinetics: Constrains on chondrule formation. In: Hewins, R., Jones, R., Scott, E. (Eds.), Chondrules and the Protoplanetary Disk. pp. 205–211.

Heim, L.-O., Blum, J., Preuss, M., Butt, H.-J., Oct. 1999. Adhesion and Friction Forces between Spherical Micrometer-Sized Particles. Physical Review Letters 83, 3328–3331.

Horányi, M., Morfill, G., Goertz, C. K., Levy, E. H., Mar. 1995. Chondrule formation in lightning discharges. Icarus 114, 174–185.

Lide, D. R. (Ed.), 1998. CRC Handbook of Chemistry and Physics. CRC Press LLC, 78th Edition.

Maharaj, S. V., Hewins, R. H., Jul. 1993. Vesicles in Experimental Chondrules as Clues to Chondrule Precursors. Meteoritics 28, 389–390.

Morfill, G., Spruit, H., Levy, E. H., 1993. Physical processes and conditions associated with the formation of protoplanetary disks. In: Levy, E. H., Lunine, J. I. (Eds.), Protostars and Planets III. pp. 939–978.

Pilipp, W., Hartquist, T. W., Morfill, G. E., Levy, E. H., Mar. 1998. Chondrule formation by lightning in the Protosolar Nebula? Astronomy & Astrophysics 331, 121–146.

Poppe, T., 2003. Sintering of highly porous silica-particle samples: analogues of early solar-system aggregates. Icarus 164, 139–148.

Poppe, T., Blum, J., Henning, T., Apr. 2000. Experiments on Collisional Grain Charging of Micron-sized Preplanetary Dust. The Astrophysical Journal 533, 472–480.

Poppe, T., Schräpler, R., 2005. Further experiments on collisional tribocharging of cosmic grains. Astronomy & Astrophysics, 1–9.

Schön, J. H., 1996. Handbook of Geophysical Exploration - Seismic Exploration. Vol. 18. Elsevier, physical Properties of Rocks - Fundamentals and Principles of Petrophysics.

Wasilewski, P., Dickinson, T., May 2000. Aspects of the validation of magnetic remanence in meteorites. Meteoritics and Planetary Science 35, 537–544.

Wasson, J. T., Mar. 1993. Multiplicity of chondrule heating events and the coarsening of chondrule textures. In: Lunar and Planetary Institute Conference Abstracts. pp. 1489–1490.

Wasson, J. T., 1996. Chondrule formation: Energetics and length scales. In: Hewins, R., Jones, R., Scott, E. (Eds.), Chondrules and the Protoplanetary Disk. pp. 45–54.

Wasson, J. T., Rubin, A. E., Jun. 2003. Ubiquitous low-FeO relict grains in type II chondrules and limited overgrowths on phenocrysts following the final melting event. Geochimica et Cosmochimica Acta 67, 2239–2250.

Wdowiak, T. J., 1983. Experimental investigation of electrical discharge formation of chondrules. In: King, E. A. (Ed.), Chondrules and their Origins. pp. 279–283.

Whipple, F. L., Jul. 1966. Chondrules: Suggestion Concerning the Origin. Science 153, 54–56.

Witt, G., Seck, H. A., 1987. Temperature History of Sheared Mantle Xenoliths from the West Eifel, West Germany: Evidence for Mantle Diapirism Beneath the Rhenish Massif. Journal of Petrology 28 (3), 475–493.